ENTROPY CONSTRAINED MULTIPLE DESCRIPTION LATTICE VECTOR QUANTIZATION

Jan Østergaard, Jesper Jensen and Richard Heusdens

Department of Mediamatics,
Delft University of Technology,
2628 CD Delft, The Netherlands,
email: {j.ostergaard, j.jensen, r.heusdens}@ewi.tudelft.nl

ABSTRACT

Recently, lattice vector quantizers (LVQ) capable of performing close to known information theoretic bounds were introduced in the area of multiple description coding (MDC). In this paper we derive analytical expressions for the central and side quantizers which minimize the expected distortion of an LVQ subject to entropy constraints on the side descriptions for given packet loss probabilities. We show that for certain packet loss probabilities, an optimal LVQ for single descriptions might not be optimal for multiple descriptions. Specifically, we show that the Z^2 lattice performs better than the A_2 lattice in some cases. Moreover, our results suggest a practical way of determining which lattice quantizers are optimal for given packet loss probabilities.

1. INTRODUCTION

Multiple description coding (MDC) aims at creating separate descriptions individually capable of reproducing a source to a specified accuracy and when combined being able to refine each other. The classical scheme involves two descriptions, see Fig. 1. The total rate is split between the two descriptions, and the distortion observed at the receiver depends on which descriptions arrive. If both descriptions are received, the distortion is lower than if only a single description is received.

The achievable rate-distortion region for the two-channel problem with respect to the Gaussian source and mean square error fidelity criterion has been known for two decades [1, 2]. The procedures leading to the achievable region were however nonconstructive, so the puzzle of designing a system capable of achieving the performance promised by theory remained unsolved. In 1993 Vaishampayan designed a practical MDC scheme for the scalar case [3]. The idea was to quantize the source by a central quantizer and then apply an index assignment algorithm that uniquely mapped all centroids of the central quantizer to centroids in two side quantizers, thereby obtaining two coarse descriptions of the source. If both descriptions were received, the inverse map was applied and the performance of the central quantizer was achieved, whereas if only one of the descriptions was received the source was reproduced at the resolution of only one of the side quantizers. The scheme developed in [3] was, however, far from the optimum rate-distortion bound. Later, Vaishampayan described an entropy constrained multiple description scalar quantization system [4] that in theory is capable of approaching the scalar MDC bound [5].

This research is supported by the Technology Foundation STW, applied science division of NWO and the technology programme of the ministry of Economics Affairs.

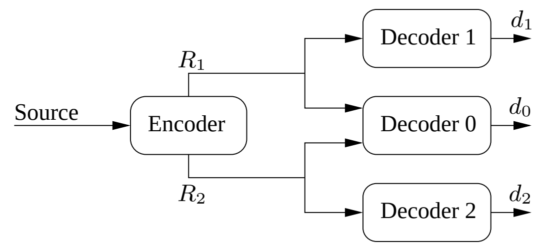

Fig. 1. The traditional two channel MDC scheme.

Recently, practical schemes that in the limit of infinite-dimensional vectors approach the theoretical rate-distortion bound have been introduced [6, 7]. Similar to [3, 4], these schemes exploit the idea of having only one central quantizer followed by an index assignment algorithm that maps each central quantizer centroid to pairs of side quantizer centroids. The scheme in [7] minimizes the central distortion given maximum allowed side distortions and side rates.

In this paper we derive analytical expressions for the central and side quantizers which minimize the expected distortion of an LVQ subject to entropy constraints on the side descriptions for given packet loss probabilities. The central and side quantizers we use are lattice quantizers as presented in [7].

2. PRELIMINARIES

The preliminaries given in this section follow directly from [7] and we refer the reader to the cited article for further details and proofs.

Let $X \in \mathcal{R}^L$ be a random vector and let $x \in \mathcal{R}^L$ denote a realization of X. Moreover, let Λ be an L-dimensional lattice in $\mathcal{R}^L$. The Voronoi cells around lattice points are congruent polytopes of volume ν and the normalized second moment of inertia of the Voronoi cell around origo is defined as

$$G(\Lambda) \triangleq \frac{1}{\nu^{2/L+1}} \int_{V_\Lambda(0)} \|x\|^2 dx,$$

where $V_\Lambda(0)$ is the Voronoi cell around origo [8].

The scheme in [7] uses an index assignment algorithm which uniquely maps all points in the central lattice (central quantizer) to pairs of points in two sublattices (side quantizers). The construction of the mapping function exploits structural properties of the lattices, making it possible to only search for the optimal mapping within a limited region, V_0, of the lattices. V_0 is shift invariant and by simply translating the mappings obtained within this region throughout $\mathcal{R}^L$, all the required mappings are found. The region V_0 is in fact the Voronoi region around origo for a product lattice, Λ_s, obtained when the two sublattices are combined. This product lattice is a scaled and rotated version of the sublattices but the shape is similar and the high-rate expressions for the side distortions in this section are based on properties of this product lattice.

The central (mean-square error) distortion obtained when both descriptions are correctly received is due to quantizing the source X using the lattice Λ and can, under a high-rate assumption, be approximated by

$$d_0 \approx G(\Lambda)\nu^{2/L}. \quad (1)$$

The side distortions, d_1 and d_2, arising when one of the descriptions is lost, can be expressed as

$$d_i \approx \frac{\gamma_j^2}{(\gamma_1+\gamma_2)^2} G(\Lambda_s) 2^{2h(X)} 2^{-2(R_1+R_2-R_0)}, \quad (2)$$

where $(i,j)=(1,2)$ or $(2,1)$ and $G(\Lambda_s)$ is the normalized second moment of the sublattices. The weight factors γ_1 and γ_2 are introduced to allow asymmetry in the distortion pair (d_1,d_2). $h(X)$ is the differential entropy of the source X and R_0 is the entropy needed for a single description system to achieve the distortion in (1) and can, under a high-rate assumption, be approximated by

$$R_0 \approx h(X) - \frac{1}{L}\log_2(\nu).$$

R_1 and R_2 are the entropies of the two side descriptions. These are expressed in bits per sample and given by

$$R_i = R_0 - \frac{1}{L}\log_2(N_i), \quad i=1,2,$$

where N_i is the index of the ith sublattice and may be seen as a redundancy factor describing the rate trade-off between central and side quantizers. In fact, N_i denotes the number of central lattice points within each Voronoi cell of the sublattices.

3. MINIMIZING AVERAGE DISTORTION

Let p_1 and p_2 denote the packet loss probabilities of description 1 and 2, respectively. The average distortion given p_1 and p_2 is then given by

$$D = \gamma_0 d_0 + \gamma_1 d_1 + \gamma_2 d_2 + \gamma E[\|X\|^2], \quad (3)$$

where we define $\gamma_0 = (1-p_1)(1-p_2)$, $\gamma_1 = (1-p_1)p_2$, $\gamma_2 = (1-p_2)p_1$ and $\gamma = p_1p_2$. We assume that p_1 and p_2 are independent.

We want to minimize the average distortion subject to entropy constraints on the two side descriptions,

$$R_i \approx h(X) - \frac{1}{L}\log_2(N_i\nu) \le R_i^*, \quad i=1,2, \quad (4)$$

where R_i^* are the entropy constraints. It follows immediately from (4) that in order to be optimal, i.e. achieve equality in (4), we must have

$$N_i\nu = 2^{L(h(X)-R_i^*)} = c_i, \quad i=1,2, \quad (5)$$

where the c_i's are constants for given target and differential entropies, so that

$$\nu = \frac{c_1}{N_1} = \frac{c_2}{N_2}, \quad (6)$$

and

$$N_1N_2 = \frac{c_1c_2}{v^2}. \quad (7)$$

With this, the average distortion (3) becomes

$$D = \gamma_0 G(\Lambda)\nu^{2/L} + (\bar{\gamma_1}+\bar{\gamma_2})G(\Lambda_s)(N_1N_2)^{2/L}\nu^{2/L} + \gamma, \quad (8)$$

where we, without loss of generality, assume X to be normalized to unit variance. The weight factors $\bar{\gamma_i}$ are given by

$$\bar{\gamma_i} = \gamma_i \frac{\gamma_j^2}{(\gamma_1+\gamma_2)^2}, \quad (9)$$

where $(i,j)=(1,2)$ or $(2,1)$.

To minimize (8) we take the derivative with respect to ν and solve the expression after equating to zero, that is,

$$\begin{aligned}\frac{\partial D}{\partial \nu} &= \frac{2}{L}\gamma_0 G(\Lambda)\nu^{2/L-1} \\ &\quad - \frac{2}{L}(\bar{\gamma_1}+\bar{\gamma_2})G(\Lambda_s)(c_1c_2)^{2/L}\nu^{-2/L-1} = 0.\end{aligned} \quad (10)$$

Hence,

$$\begin{aligned}\nu &= \left(\frac{G(\Lambda_s)}{G(\Lambda)}\right)^{L/4}\left(\frac{\bar{\gamma_1}+\bar{\gamma_2}}{\gamma_0}\right)^{L/4}\sqrt{c_1c_2} \\ &= \sqrt{c_1c_2}\left(\frac{G(\Lambda_s)}{G(\Lambda)}\right)^{L/4}\left(\frac{p_1p_2}{p_1+p_2-2p_1p_2}\right)^{L/4}, \end{aligned} \quad (11)$$

so that, by (6), the individual index values are given by

$$N_i = \sqrt{\frac{c_i}{c_j}}\left(\frac{G(\Lambda)}{G(\Lambda_s)}\right)^{L/4}\left(\frac{p_1+p_2-2p_1p_2}{p_1p_2}\right)^{L/4}. \quad (12)$$

For the balanced case where the entropy constraints are equal, that is, $c^2=c_1c_2$ and equal packet loss probabilities $p_1=p_2=p$, we get

$$\nu = c\left(\frac{G(\Lambda_s)}{G(\Lambda)}\right)^{L/4}\left(\frac{p}{2(1-p)}\right)^{L/4}. \quad (13)$$

In this case, the index values will be equal as well and (12) reduces to

$$N = \left(\frac{G(\Lambda)}{G(\Lambda_s)}\right)^{L/4}\left(\frac{2(1-p)}{p}\right)^{L/4}. \quad (14)$$

Eqs. (11) and (12) (and (13) and (14) for the balanced case) show, for given p_1 and p_2, how to compute the optimal ν and N_i which completely characterize the central and side quantizers.

4. ADMISSIBLE VALUES OF N_I

Eqs. (13) and (14) suggest that we are able to continuously trade-off central versus side-distortion by adjusting N_i and ν according to the packet loss probability. This is, however, not the case, since certain constraints must be put on N_i to make sure that we obtain proper sublattices [7]. First of all, since N_i denotes the number of central lattice points within each Voronoi cell of the sublattices, it must be integer. Secondly, a proper sublattice is for example a sublattice which is geometrical similar to the central lattice, i.e. it

Name	Dim.	N_i
Z	1	1,3,5,7,9,...
Z^2	2	1,5,9,13,17,25,29,37,41,45,49,...
A_2	2	1,7,13,19,31,37,43,49,...
D_4	4	1,25,49,169,289,625,...
Z^4	4	1,25,49,81,121,169,225,289,361,...

Table 1. Index values that give geometrical similar and clean sublattices for different central lattices in one, two and four dimensions.

can be obtained from the central lattice by applying a change of scale, a rotation and possibly a reflection. The normalized second moment is independent of scaling, rotation and reflection [8], so by using sublattices which are geometrical similar to the central lattice, the ratio of the normalized second moments is equal to one.

For any proper sublattice, a number of central lattice points will be located within each Voronoi cell of sublattice points and perhaps on the boundaries between neighboring Voronoi cells. To obtain an injective mapping from central lattice points to sublattice points, thereby making it possible to reconstruct in a unique way to the central lattice points when both descriptions are received, it is required that each central lattice point is associated with one and only one sublattice point from each sublattice. In situations where central lattice points are on the boundary of sublattice Voronoi cells, ties must be broken. Tie breaking will in general influence the shape of a Voronoi cell, i.e. change it from that specified by the sublattice. A change of shape of the Voronoi cell affects the normalized second moment, hence the "quality" of the reconstructed source is affected. Sublattices having no central lattice points on the boundary of their Voronoi cells are called clean. In [9] partial answers are given to when a central lattice contains a sublattice of index N_i that is geometrical similar to the central lattice, and necessary and sufficient conditions are given for any central lattice in two dimensions to contain a geometrical similar and clean sublattice of index N_i. These results are extended in [7] to geometrical similar and clean sublattices in four dimensions for the Z^4 and D_4 lattice. In addition, results are given for any Z^L lattice where $L = 4k, k \geq 1$. Table 1 briefly summarizes admissible N_i values for the known cases. As a consequence, for the balanced case, an index value of unity (maximum redundancy) is always optimal for $p \geq 2/3$, independent of the dimension of the source whenever geometrical similar lattices are being used. This can be seen by rewriting (14) as

$$p = \frac{2}{\frac{G(\Lambda_s)}{G(\Lambda)} N^{4/L} + 2}, \qquad (15)$$

where $N \geq 1$.

5. RESULTS

In this section we present theoretical and experimental results obtained by computer simulations for the balanced case. We quantized a two-dimensional unit variance Gaussian source using the A_2 and the Z^2 quantizers (lattices) at an entropy of 3 bits/sample per description. Fig. 2 shows the theoretical average distortion obtained with the A_2 quantizer when varying N continuously according to (14) as well as for different fixed values of N taken from Table 1. The thick bottom line in the figure indicates the

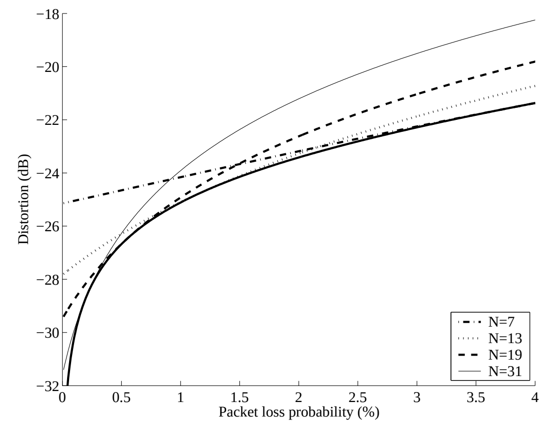

Fig. 2. Average distortion when the A_2 quantizer is used on a two-dimensional unit variance Gaussian source.

lower convex hull (LCH) obtained when N follows (14). Since N is restricted to the values given in Table 1, we cannot reach the LCH for all values of p.

For single description systems and mean-squared error distortion criterion, the A_2 quantizer is known to be optimal in two dimensions [8]. For the multiple description system considered here, this is not always the case as the following example illustrates. Each index value in Table 1 results in a different average distortion (when the entropy is kept constant) for a given quantizer. For each packet loss probability we use that index value which gives the lowest average distortion. This gives rise to an operational lower convex hull (OLCH) for each quantizer. In Fig. 3 is shown the difference between the OLCH and the LCH for the A_2 quantizer. Keep in mind that the LCH is obtained when N follows (14). Inserting the N values from Fig. 2 into (15), we find that they are optimal for $p \approx 0.21\%, 0.55\%, 1.17\%$ and 3.9%, which is where the dips occur for A_2 in Fig. 3. Also shown in Fig. 3 is the performance curve obtained for the Z^2 quantizer, when subtracting the LCH from the OLCH of the Z^2 quantizer. The dotted line indicate the 0.1671 dB difference between the quantizers (dimensionless) normalized second moments [8] and for low packet loss probabilities we expect to approximately achieve this distortion gain whenever equivalent index values for the two quantizers are obtainable. As the packet loss probability is increased the gain decreases and approaches zero as $p \to 1$. However, in Fig. 3, we notice that for $p \approx 2.2\%$ the distortion when using Z^2 is lower than when using A_2. For $p \approx 20\%$ this phenomenon is even more apparent (not shown in the figures). These deviations occur whenever allowed index values for Z^2 gets closer to the optimal index value than what is possible for A_2 indices. In these situations, it is better to use the Z^2 quantizer than the A_2 because the increase in distortion for the A_2 caused by using index values far away from optimal values, is greater than the actual decrease in distortion caused by A_2's lower normalized second moment.

In order to obtain experimental results, we used 20 realizations of length 10^5 of a two-dimensional unit-variance independent identically distributed Gaussian source. For different values of p and admissible values of N, we designed optimal quantizers by computing ν according to (13) to satisfy an entropy constraint of 3 bits/sample per description. Figure 4 shows both ex-

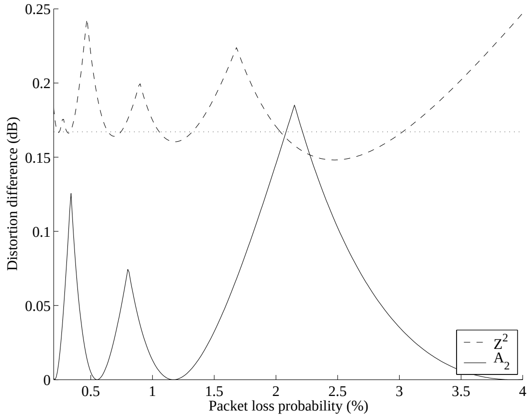

Fig. 3. The LCH is here subtracted from the OLCH of the A_2 and Z^2 quantizers. Dips occur whenever obtainable N values from Table 1 are optimal.

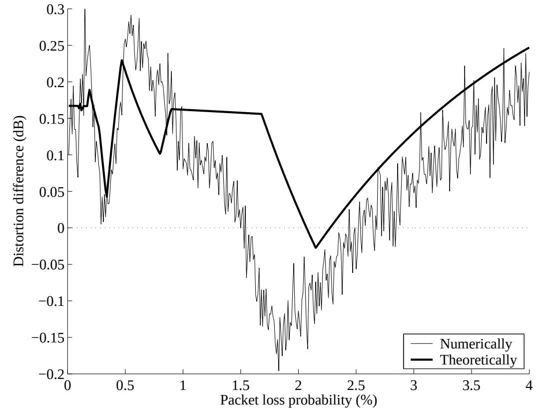

Fig. 4. The difference between the OLCH of the Z^2 quantizer and the A_2 quantizer.

perimentally and theoretically obtained OLCH's for the Z^2 and A_2 quantizers. The graphs are obtained by subtracting the OLCH of the Z^2 quantizer from the OLCH of the A_2 quantizer. Whenever the curves becomes negative, i.e. below the dotted line, the Z^2 quantizer performs better than the A_2 quantizer. We see that the Z^2 quantizer indeed performs better than the A_2 quantizer around $p = 2\%$. Especially for high index values, i.e. low packet loss probabilities, there is a good match between theory and the numerically obtained results.

In four dimensions, we compared the OLCH of the D_4 quantizer [8] with the OLCH of the Z^4 quantizer. From Table 1 we see that the Z^4 quantizer has more index values than the D_4 quantizer within a given range, so we expect the performance loss, caused by using suboptimal index values, to be greater for the D_4 quantizer than for the Z^4 quantizer. The greatest performance loss for the D_4 quantizer is around 0.2 dB. Since the difference in (dimensionless) normalized second moments between the two quantizers is 0.3657 dB [8], D_4 is always better than Z^4. Other four dimensional quantizers might be considered, e.g. a product quantizer constructed by combining two A_2 quantizers. However, finding allowed index values for other four dimensional quantizers and determining their performance in comparison with that of D_4 is a topic for future research.

6. CONCLUSION

In this work we derived analytical expressions for the central and side quantizers which minimize the expected distortion of an LVQ subject to entropy constraints on the side descriptions for given packet loss probabilities. We showed that, for certain packet loss probabilities, the Z^2 quantizer performs better than the A_2 quantizer. Our results suggest a practical way of determining which lattice quantizers are optimal for given packet loss probabilities.

7. REFERENCES

[1] L. Ozarow, "On a source-coding problem with two channels and three receivers," *Bell System Technical Journal*, vol. 59, pp. 1909–1921, December 1980.

[2] A. A. El Gamal and T. M. Cover, "Achievable rates for multiple descriptions," *IEEE Trans. Inform. Th.*, vol. IT-28, no. 6, pp. 851–857, November 1982.

[3] V. A. Vaishampayan, "Design of multiple description scalar quantizers," *IEEE Trans. Inform. Th.*, vol. 39, no. 3, pp. 821–834, May 1993.

[4] V. A. Vaishampayan and J. Domaszewicz, "Design of entropy-constrained multiple-description scalar quantizers," *IEEE Trans. Inform. Th.*, vol. 40, no. 1, pp. 245–250, January 1994.

[5] V. A. Vaishampayan and J.-C. Batllo, "Asymptotic analysis of multiple description quantizers," *IEEE Trans. Inform. Th.*, vol. 44, no. 1, pp. 278–284, January 1998.

[6] V. A. Vaishampayan, N. J. A. Sloane, and S. D. Servetto, "Multiple-description vector quantization with lattice codebooks: Design and analysis," *IEEE Trans. Inform. Th.*, vol. 47, no. 5, pp. 1718–1734, July 2001.

[7] S. Diggavi, N. J. A. Sloane, and V. A. Vaishampayan, "Asymmetric multiple description lattice vector quantizers," *IEEE Trans. Inform. Th.*, vol. 48, no. 1, pp. 174–191, January 2002.

[8] J. H. Conway and N. J. A. Sloane, *Sphere packings, Lattices and Groups*, Springer, 3rd edition, 1999.

[9] J. H. Conway, E. M. Rains, and N. J. A. Sloane, "On the existence of similar sublattices," *Canadian Jnl. Math.*, vol. 51, pp. 1300–1306, 1999.